

Review began 10/15/2024

Review ended 11/22/2024

Published 12/30/2024

© Copyright 2024

Desai. This is an open access article distributed under the terms of the Creative Commons Attribution License CC-BY 4.0., which permits unrestricted use, distribution, and reproduction in any medium, provided the original author and source are credited.

DOI: <https://doi.org/10.7759/s44388-024-00429-2>

Studies on Structural, Morphological and Optoelectrical Properties of Spray-Deposited Iron-Doped Cadmium Oxide Thin Films

Sandeep P. Desai¹

1. Department of Basic Sciences and Engineering, KIT's College of Engineering, Kolhapur, IND

Corresponding author: Sandeep P. Desai, swayamswaraj@gmail.com

Abstract

Cadmium-based transparent conductive oxides have received much attention due to their exceptional carrier concentrations, almost metallic conductivities and simple rock salt-like crystal structure. In the present study, the effect of iron (Fe) doping on physicochemical and opto-electrical properties of spray-deposited cadmium oxide (CdO) thin film was studied by varying the doping concentration of Fe. The X-ray diffraction (XRD), field emission scanning electron microscopy (FE-SEM), UV-Vis spectroscopy, photoluminescence (PL) study and electrical properties using the Hall effect in Van der Pauw configuration were used to study the different physicochemical and optoelectrical properties of Fe-doped CdO thin films. The XRD patterns studied for Fe:CdO films show a polycrystalline nature and the crystallite size increases with an increase in doping concentration. FE-SEM images show an interconnected chain structure. The thickness of the films increases with an increase in doping concentration of Fe, as more nucleation sites are available. A transmittance of 76% was recorded at 550 nm wavelength for 4 at% doped Fe:CdO films. The direct band gap increases from 2.62 eV to 2.83 eV as the Fe doping concentration increases from 1 at% to 4 at% Fe:CdO films and further decreases to 2.71 eV. The PL spectrum indicates two emission peaks at 434.19 nm and 539.61 nm significantly. The electrical measurements show that Fe doping concentration in CdO film increases, the sheet resistance decreases from $2.89 \Omega^{-1}$ to $2.06 \Omega^{-1}$, which is attributed to the increase in mobility of carriers. The maximum mobility of $94.26 \text{ cm}^2/\text{Vs}$ is obtained for 4 at% Fe:CdO thin film. The figure of merit (Φ), a factor significant for opto-electronic applications, was found to vary between $3.40 \times 10^{-3} \Omega^{-1}$ and $31.16 \times 10^{-3} \Omega^{-1}$ for Fe: CdO films.

Categories: Advanced Materials, Materials Engineering, Nano Materials**Keywords:** carrier concentration, mobility

Introduction

Transparent conducting oxides (TCOs) are promising candidates in technologies that require both high transparency and good electrical conductivity. Wide band gap metal oxides are one of the preferred choices for the synthesis of TCOs. New materials must be developed with lower resistivities and higher optical transparencies for the next generation of TCOs [1-4]. Out of the different TCO materials, cadmium-based TCOs have received much attention due to their superior carrier concentrations, nearly metallic conductivities, high optical transparencies and relatively simple cubic rock salt crystal structure [5]. CdO thin films have high transparency (>75%) in the visible region of the electromagnetic spectrum and show degenerate n-type conductivity, mainly due to oxygen vacancies and Cd interstitials, as well as a high carrier concentration of about $10^{20}/\text{cm}^3$. The smaller carrier effective mass ($0.21 \pm 0.01m_0$) in CdO makes it an ideal material for doping studies. Though the E_g of bulk CdO is ~2.3 eV, which restricts the optical transparency, doping offers the possibility of tuning the electronic structure and the E_g through a carrier concentration-dependent Moss-Burstein (MB) energy level shift. Additionally, its low effective carrier mass efficiently increases the bandgap for heavily doped CdO films to as high as 3.35 eV [6,7]. Dhakel has extensively studied the effect of different dopants like, Eu, Sm, Ga, Tl, Gd, etc., on the optoelectrical and structural properties of CdO thin films deposited by vacuum evaporation technique [8-12]. It has been reported that the ionic radius and the properties of doped ions change the electrical and optical properties of CdO thin films. The properties of TCO materials derive from the nature, number and atomic arrangements of metal cations in crystalline or amorphous oxide structures, from the resident morphology, and from the presence of intrinsic or intentionally introduced defects. In the present study, the effect of iron (Fe) doping on physicochemical and optoelectrical properties of spray pyrolytically deposited CdO thin film is studied systematically.

Materials And Methods

Thin films of Fe-doped CdO (Fe:CdO) were deposited on preheated soda lime glass (SLG) substrate using

How to cite this article

Desai S P (December 30, 2024) Studies on Structural, Morphological and Optoelectrical Properties of Spray-Deposited Iron-Doped Cadmium Oxide Thin Films. Cureus J Eng 1 : es44388-024-00429-2. DOI <https://doi.org/10.7759/s44388-024-00429-2>

chemical Spray Pyrolysis Technique. The deposition parameters, like substrate temperature (350°C), spray rate (5 ml/min), nozzle to substrate distance (30 cm) and pressure of carrier gas (75 kg/cm²), were kept constant [5]. The CdO thin films deposited with different Fe concentrations (1% to 5%) were denoted as F₁, F₂, F₃, F₄ and F₅ for further reference. It has been observed that when solution is sprayed on preheated SLG substrate, pyrolytic decomposition of solution takes place and yellowish brown color films are deposited. The structural properties were studied by X-ray powder diffractometer [Bruker AXS (D2-Phaser) USA] using Cu Kα (λ = 1.54056 Å) operated at 30 kV, 20 mA. The microstructural study was carried out using field emission scanning electron microscopy (FE-SEM) (Make:Hitachi S-4800, Japan). The thickness of the thin films was obtained from the cross-sectional FE-SEM images. The transmission and optical absorption spectra were studied at room temperature within 200-800 nm wavelength range using a UV-Vis spectrophotometer (Make:Shimadzu UV-1800, Japan). The photoluminescence spectra were recorded using spectrofluorometer (Make:Fluoromax-4, Japan). The room temperature electrical measurements were carried out with a Hall Effect set up in van-der Pauw configuration (Make:SES Instruments Pvt. Ltd, Roorkee, India).

Results

X-ray diffraction (XRD) study

The XRD patterns of the Fe:CdO thin films deposited with different Fe doping concentrations (1 at% to 5 at%) are shown in Figure 1. All the Fe:CdO thin films show polycrystalline textures. Crystal growth is observed to be more preferential along (111), (200) and (220) planes. The obtained result confirms the phase-pure face-centered cubic structure of Fe:CdO thin films, which matches with the JCPDS Card No. 01-075-0592 [13].

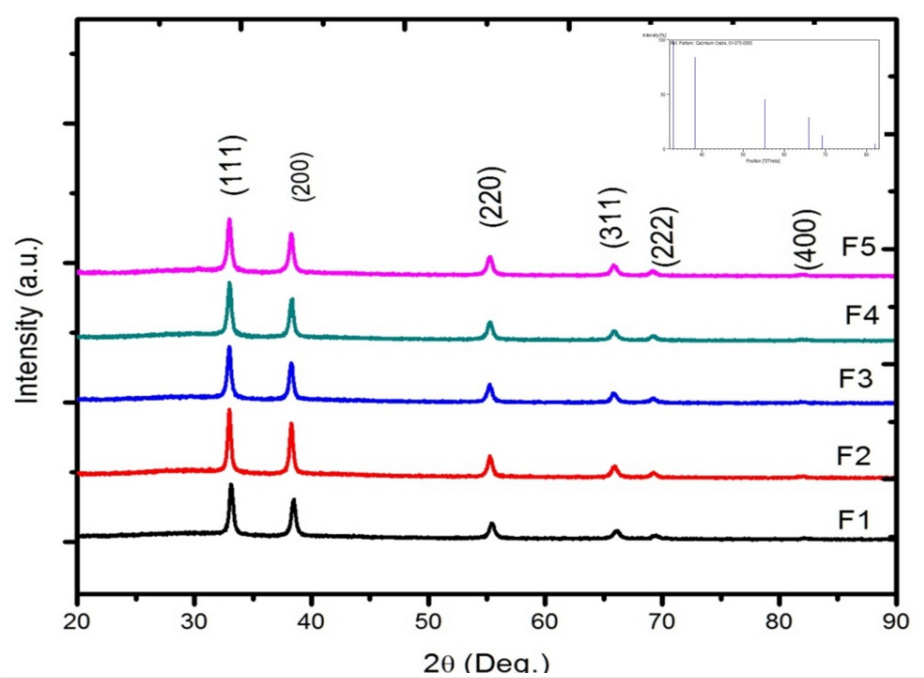


FIGURE 1: XRD patterns of Fe:CdO thin films
XRD, X-ray diffraction

From XRD, it is confirmed that Fe³⁺ ions successfully substituted Cd²⁺ ions in CdO lattice as there are no impurity peaks observed and there is no secondary phase formed. The crystallite size of different planes was estimated using Scherrer's equation [14],

$$D = \frac{0.9\lambda}{\beta \cos\theta} \dots\dots\dots(1)$$

Where, D is the crystallite size, θ is the diffraction angle, λ is the wavelength of X-rays and β is full width at half maxima (FWHM). The calculated crystallite size (D) for all Fe:CdO thin films is given in Table 1. It is found that the crystallite size varies as 23.5 nm, 26.4 nm, 27 nm, 33.2 nm and 27.7 nm with increasing doping

concentration of Fe from 1 at% to 5 at% in CdO films. The increase in the crystallite size is attributed to the better crystallinity due to the proper occupation of Fe atoms at regular sites in the CdO lattice, whereas the decrease in crystallite size for 5 at% doped Fe:CdO thin film may be due to saturation of Fe in CdO samples.

| Fe:CdO at% | Bragg's angle (2θ) | Miller indices (hkl) | Lattice constant a (Å) | Texture coefficient (TC) | Strain ε (×10 ⁻³) | Crystallite size D (nm) | Average D (nm) |
|------------|--------------------|----------------------|------------------------|--------------------------|-------------------------------|-------------------------|----------------|
| 1 | 33.14 | 111 | 4.68 | 1.4 | 3.19 | 26.3 | 23.5 |
| | 38.5 | 200 | 4.67 | 1.35 | | 26.7 | |
| | 55.43 | 220 | 4.68 | 1.02 | | 22.8 | |
| | 66.08 | 311 | 4.68 | 0.79 | | 34.3 | |
| | 69.48 | 222 | 4.68 | 0.88 | | 17.5 | |
| 2 | 32.98 | 111 | 4.7 | 1.38 | 2.6 | 26.3 | 26.4 |
| | 38.28 | 200 | 4.7 | 1.42 | | 23.7 | |
| | 55.24 | 220 | 4.7 | 1.02 | | 20.7 | |
| | 65.95 | 311 | 4.69 | 0.84 | | 20 | |
| | 69.22 | 222 | 4.7 | 0.85 | | 49.1 | |
| 3 | 32.99 | 111 | 4.7 | 1.38 | 2.57 | 30 | 27 |
| | 38.29 | 200 | 4.7 | 1.17 | | 30.5 | |
| | 55.21 | 220 | 4.7 | 1 | | 25.3 | |
| | 65.78 | 311 | 4.7 | 0.8 | | 24 | |
| | 69.22 | 222 | 4.7 | 0.86 | | 24.5 | |
| 4 | 33.01 | 111 | 4.69 | 1.41 | 1.46 | 30 | 33.2 |
| | 38.32 | 200 | 4.69 | 1.17 | | 26.7 | |
| | 55.3 | 220 | 4.69 | 0.98 | | 45.5 | |
| | 65.84 | 311 | 4.7 | 0.86 | | 40 | |
| | 69.22 | 222 | 4.7 | 0.83 | | 35 | |
| 5 | 32.98 | 111 | 4.7 | 1.39 | 1.46 | 30 | 27.7 |
| | 38.24 | 200 | 4.7 | 1.19 | | 26.7 | |
| | 55.27 | 220 | 4.7 | 1.03 | | 20.7 | |
| | 65.79 | 311 | 4.7 | 0.85 | | 40 | |
| | 69.31 | 222 | 4.69 | 0.8 | | 35 | |

TABLE 1: The values of Bragg's angle (2θ), Miller indices (hkl), lattice constant (a), texture coefficient (TC), strain (ε), crystallite size (D) of 1 at% to 5 at% Fe:CdO thin films

To describe this preferred orientation of crystal growth, the texture coefficient TC(hkl) for all the planes was calculated using the expression [14],

$$TC(hkl) = \frac{\frac{I(hkl)}{I_o(hkl)}}{\frac{1}{N} \sum \frac{I(hkl)}{I_o(hkl)}} \dots\dots\dots(2)$$

where, $TC(hkl)$ is the texture coefficient of the (hkl) plane, $I(hkl)$ is the measured intensity of the peak, I_0 is the standard intensity of the (hkl) plane from JCPDS data (JCPDS card No. 01-075-0592) and N is the number of reflection peaks observed. From the TC measured for various planes for films deposited at different Fe concentrations, it is clear that all films have preferential orientation along the (111) and (200) planes.

The inherent strain and stress are generated in the films due to interlayer lattice mismatch during the growth of the film, deficiencies and defects generated in the film, like edge dislocation, screw dislocation and void spaces, etc., due to which the unit cell of the crystal structure gets deformed, resulting in the development of strain [14]. The strain in the sample can be determined by using the equation

$$\beta = \frac{\lambda}{D \cos \theta} - \varepsilon \tan \theta \quad \dots\dots\dots(3)$$

where, β is the FWHM, λ is the wavelength of X-ray, D is the crystallite size, ε is the strain in the sample and θ is the Bragg's angle. Here by plotting the graph of $(\beta \cos \theta)/\lambda$ vs $\sin \theta/\lambda$ and taking slope of it, the average strain is calculated. It is observed that strain decreases with an increase in doping concentration in Fe:CdO thin films. The variation in strain is due to the crystallite size variation, which influences grain size, which consequently influences the grain boundaries [15].

Field emission scanning electron microscopy (FE-SEM)

Surface morphology and film thickness are examined by FE-SEM images and are presented in Figure 2. It is observed that the Fe:CdO thin films are homogeneous, crack-free, showing compact granular morphology, which credits to the uniform growth of film during pyrolytic decomposition. FE-SEM images of 1 at% Fe:CdO show interconnected, larger-size granular structures with a number of voids, which are reduced at higher Fe doping concentrations. As the doping concentration increases, it is seen that the thickness of the film increases from 576 nm to 1517 nm; this may be due to the higher growth rate possible with increased Fe doping. The film morphology also changes; it becomes more compact, and the size of granules also decreases. The spherical, peanut-like interconnected crystallites are observed for 4 at% and 5 at% Fe:CdO thin films.

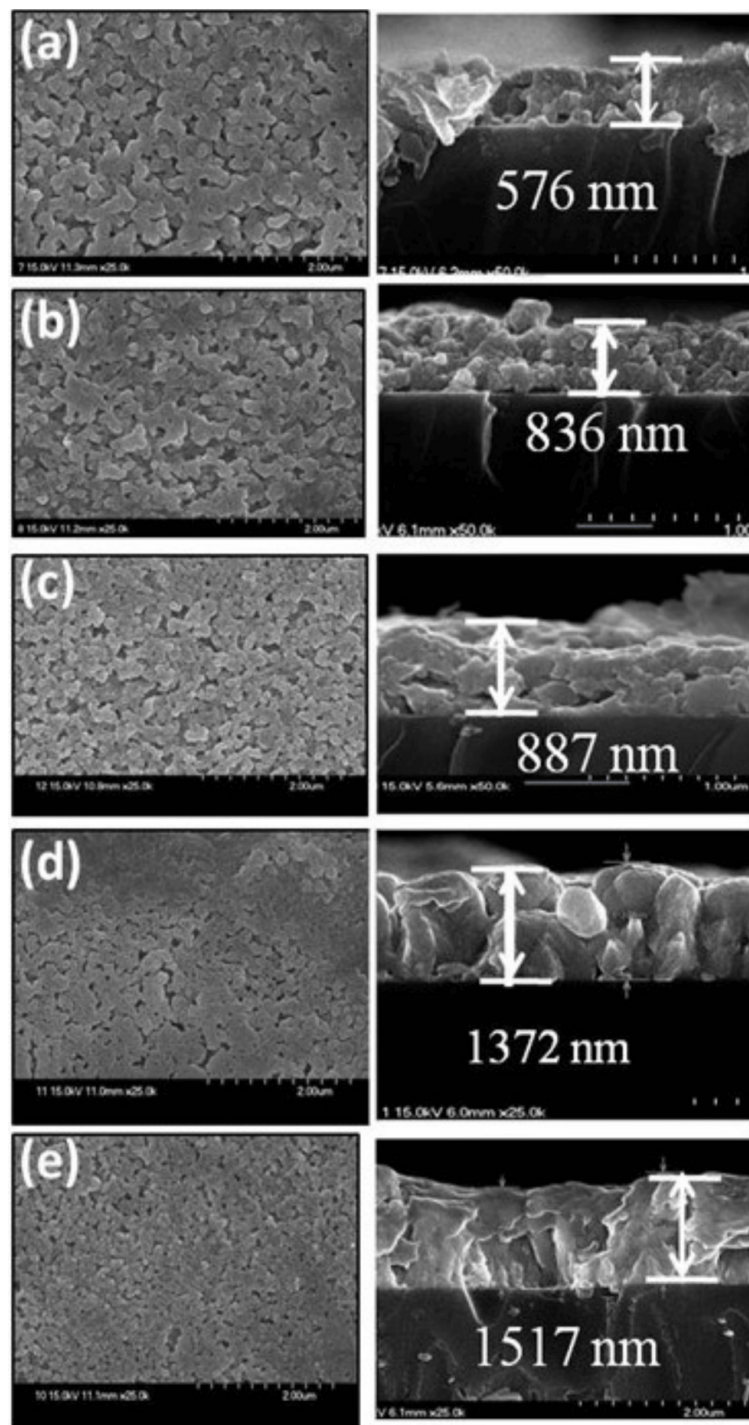


FIGURE 2: FE-SEM and cross-sectional images of Fe:CdO thin films deposited at 350°C

FE-SEM, field emission scanning electron microscopy

Optical properties

Transmittance spectra of Fe:CdO film are shown in Figure 3. It is observed that the transmittance increased from 63% to 76% with an increase in Fe doping from 1 at% to 4 at%, and further decreased to 72% for 5 at% Fe:CdO thin film. It is well known that the transmittance depends on crystallinity factor and since it is higher for 4 at% Fe:CdO thin film, it shows a maximum transmittance of 76% measured at 550 nm. The optical band gap values are determined from Tauc plot, i.e. $(\alpha h\nu)^2$ vs $(h\nu)$ graph, and by extrapolating the linear portion of the graph on the $h\nu$ axis at $\alpha = 0$. The values of direct band gap increase from 2.62 eV to 2.83 eV as the Fe doping concentration increases from 1 at% to 4 at% Fe:CdO films, and further it decreases

to 2.71 eV. This decrease in bandgap of Fe:CdO film is attributed to an increase in carrier concentration, which leads to the MB effect [16]. The MB effect is a phenomenon in semiconductor physics that typically occurs when the Fermi level is pushed above the conduction band due to an increased carrier concentration, leading to a narrowing of the optical bandgap. The variation of the optical band gap with the Fe concentration is shown in Figure 4.

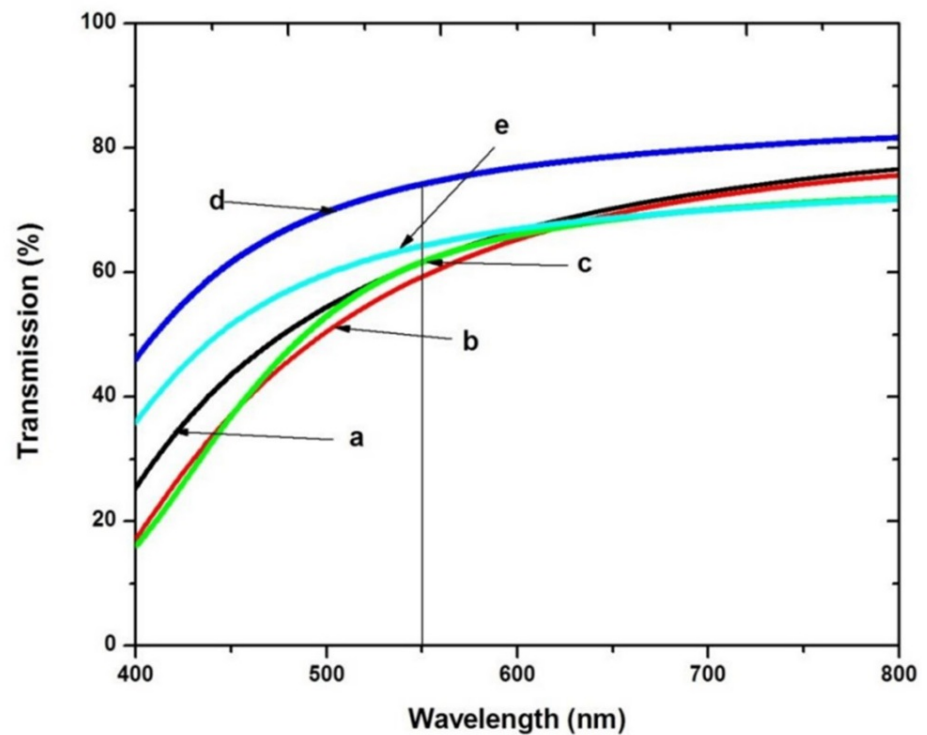


FIGURE 3: Transmittance spectra of (a) 1 at% to (e) 5 at% Fe:CdO thin film deposited at 350°C substrate temperature

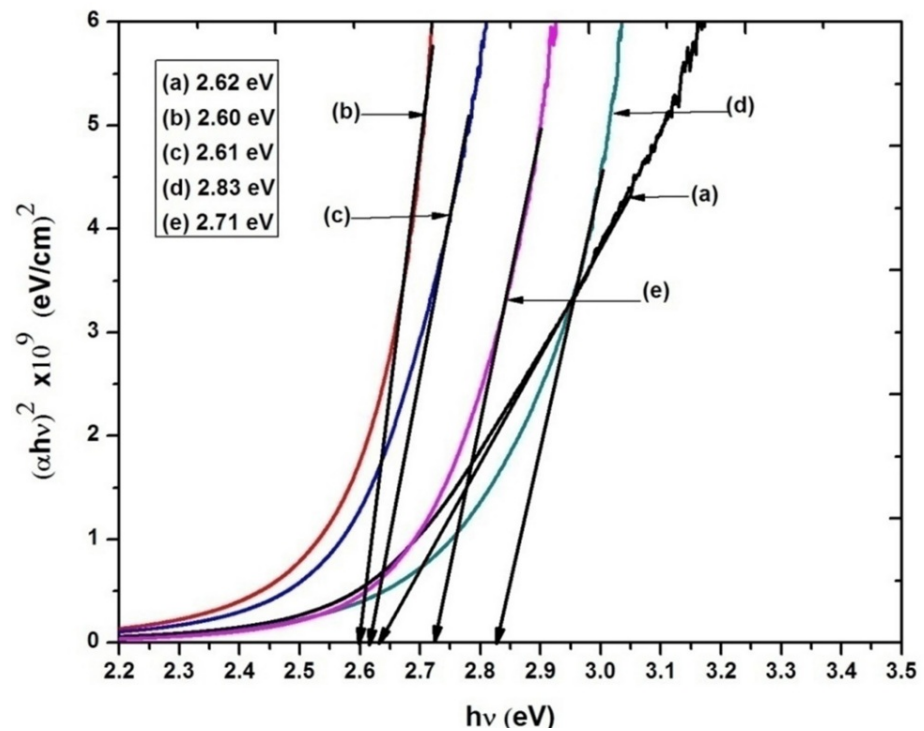


FIGURE 4: The plots of $(\alpha h\nu)^2$ vs $h\nu$ for Fe:CdO thin films of different Fe doping concentrations deposited at 350°C substrate temperature

Photoluminescence (PL) study

PL spectroscopy is used to determine the optical quality of Fe:CdO films. The room temperature PL spectra of 1 at% to 5 at% Fe doped samples are shown in Figure 5 after excitation at 400 nm (blue). Two emission peaks at 434.19 nm and 539.61 nm (green) are observed significantly for 4 at% Fe doped Fe:CdO films; this may be due to the combination of electrons and holes from the conduction band and valance band, whereas for other Fe:CdO films, the peak intensity is less [17].

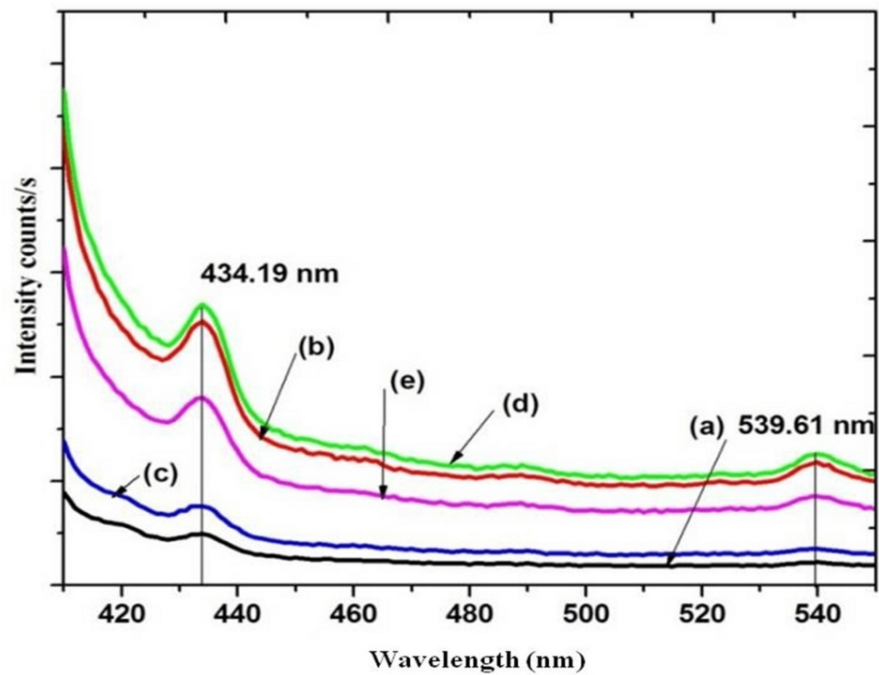


FIGURE 5: PL spectra of Fe:CdO films (a) 1 at%, (b) 2 at%, (c) 3 at%, (d) 4 at% and (e) 5 at% Fe, deposited at 350°C substrate temperature
PL, photoluminescence

Electrical properties

The values of sheet resistance (R_s), transmittance (T), figure of merit (f), resistivity (ρ), carrier concentration (n), mobility (μ), Fermi energy (E_F) and IR reflectivity of 1 at% to 5 at% Fe:CdO thin films deposited at 350°C substrate temperature are depicted in Table 2.

| Fe:CdO (at%) | R_s (Ω) | T (%) | $\Phi \times 10^{-3}$ (Ω^{-1}) | $\rho \times 10^{-4}$ ($\Omega.cm$) | $n \times 10^{20}$ (cm^{-3}) | μ (cm^2/Vs) | E_F (eV) | $n^{2/3} 10^{13}$ (cm^{-2}) | μ_{cal} (cm^2/Vs) | IR (%) |
|--------------|--------------------|-------|---|---------------------------------------|----------------------------------|---------------------|------------|---------------------------------|---------------------------|--------|
| 1 | 2.89 | 63 | 3.40 | 1.67 | 6.00 | 62.37 | 1.389 | 7.11 | 13.81 | 96.99 |
| 2 | 2.63 | 68 | 8.01 | 2.20 | 4.49 | 63.07 | 1.144 | 5.86 | 16.75 | 97.25 |
| 3 | 2.30 | 72 | 16.27 | 2.03 | 4.24 | 72.63 | 1.101 | 5.64 | 17.40 | 97.60 |
| 4 | 2.06 | 76 | 31.16 | 2.83 | 2.34 | 94.26 | 0.741 | 3.79 | 25.86 | 97.84 |
| 5 | 2.84 | 72 | 13.15 | 4.32 | 3.49 | 41.43 | 0.967 | 4.95 | 19.81 | 97.04 |

TABLE 2: The values of sheet resistance (R_s), transmittance (T), figure of merit (Φ), resistivity (ρ), carrier concentration (n), mobility (μ), Fermi energy (E_F), IR reflectivity (IR) of 1 at% to 5 at% Fe:CdO thin films deposited at 350°C substrate temperature

In the present case, it is observed that the mean free path for 1 at% to 5 at% Fe:CdO films calculated are 23.71 nm, 26.12 nm, 26.62 nm, 32.46 nm and 28.41 nm, and the crystallite size values are 23.5 nm, 26.4 nm, 27 nm, 33.2 nm and 27.7 nm, respectively, which are nearly the same. Therefore, it is concluded that the

grain boundary scattering mechanism is the dominant phenomenon in the case of Fe:CdO for the improvement in mobility of charge carriers. The maximum mobility of 94.26 cm²/Vs is obtained for 4 at% Fe:CdO thin film. The variation of carrier concentration and mobility with increasing Fe doping in CdO thin film is plotted and shown in Figure 6. The electrical parameters obtained show similar trends as studied by Sankarasubramanian et al. [18], i.e. the resistivity decreases up to the optimized dopant concentration and further increases. The mobility and carrier concentration were increased and then found to be decreased.

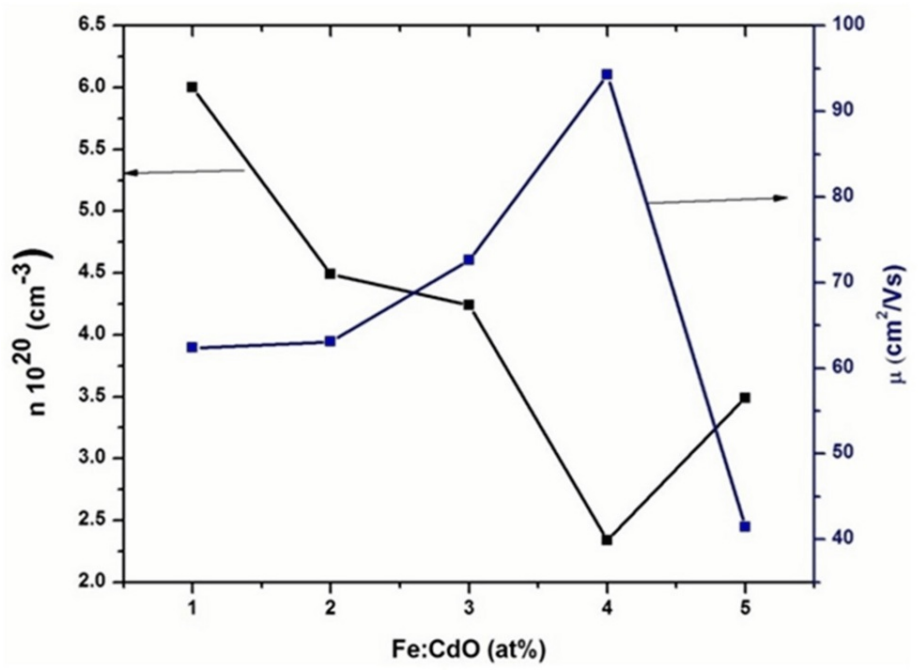


FIGURE 6: Carrier concentration and mobility of Fe:CdO thin films of different Fe doping (1 at% to 5 at%) deposited at 350°C substrate temperature

As Fe doping concentration in CdO film increases, the sheet resistance decreases from 2.89 Ω⁻¹ to 2.06 Ω⁻¹, which is attributed to the increase in mobility of carriers. The eventual increase in sheet resistance for 5 at% Fe:CdO thin film to 2.84 Ω may be due to the fact that when Fe exceeds the limit of maximum solubility in CdO thin films, it produces a grain boundary segregation of impurities, which causes a dispersion of carriers. From an application point of view for TCO to be used in various optoelectronic devices, figure of merit (Φ) is one of the very important parameters. The variation of figure of merit with increasing Fe doping is calculated from Haacke's formula [19].

$$\phi = \frac{T^{10}}{R_s} \dots\dots\dots(4)$$

Where, ϕ is figure of merit, T is the transmittance and R_s is the sheet resistance. The figure of merit values of Fe:CdO thin films are presented in Table 2 and its variation is shown in Figure 7 with increasing Fe doping concentration in CdO thin films. The figure of merit increases with Fe doping concentration, and it reaches its maximum for the 4 at% Fe:CdO film, which is 31.16 × 10⁻³ (Ω)⁻¹ due to its high transmittance and low sheet resistance.

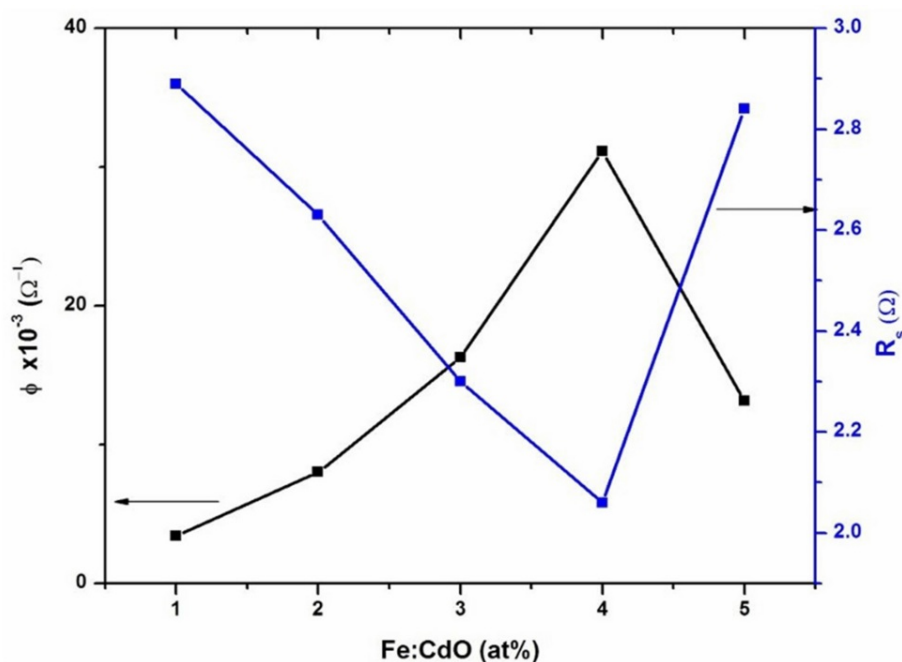


FIGURE 7: Variation of figure of merit and sheet resistance of Fe:CdO thin films deposited at substrate temperature of 350°C substrate temperature

Discussion

The properties of TCO materials derive from the nature, number and atomic arrangements of metal cations in crystalline or amorphous oxide structures, from the resident morphology and from the presence of intrinsic or intentionally introduced defects. In this study, the effect of Fe doping on the CdO thin films has been studied. It is observed that the structural, morphological and optoelectrical properties of Fe doped CdO thin films vary with the doping concentration. Keeping spray deposition parameters constant, it is observed that the 4 at% Fe:CdO thin films show better optoelectrical properties. It can be attributed to several factors related to the electronic structure, doping concentration and interaction between the Fe dopant and the host material CdO. Doping CdO with Fe introduces additional free carriers (electrons) due to the presence of iron ions. At low doping concentrations, Fe acts as a donor, enhancing the conductivity of CdO. The optimal concentration of 4 at% Fe might provide the right balance of extra charge carriers without leading to excessive scattering or other negative effects that could occur at higher concentrations.

Conclusions

Doping can enhance the optoelectrical properties of metal oxide thin films which will be applicable in technological demands wherein it is required to have very good transparency along with good conductivity. Iron-doped cadmium oxide thin films show better optoelectrical properties, like high transmittance (76%), band gap nearly 2.83eV, very low sheet resistance (2.06 Ω), high mobility (94.26 cm²/Vs) and very good figure of merit $31.16 \times 10^{-3} (\Omega)^{-1}$ for 4 at% Fe-doped CdO thin films, these properties make it one of the suitable candidates in applications like front-surface electrodes for solar cells and flat-panel displays, touch panels, and sensors, etc.

Future studies could explore a wide variety of dopants to fine-tune the carrier concentration and mobility. Optimizing doping concentrations and the methods used to incorporate these dopants could lead to CdO films with more controlled conductivity, for a specific application. One of the challenges with CdO is its instability under high temperature or in the presence of moisture. Doping CdO may potentially improve its structural stability, which is critical for long-term reliability in devices like solar cells and transparent displays. Additionally, CdO-based TCOs could be integrated with other novel materials, such as organic semiconductors, graphene or MoS₂, and perovskite materials, wherein doping may optimize the interfaces and improve the overall device performance.

Additional Information

Author Contributions

All authors have reviewed the final version to be published and agreed to be accountable for all aspects of the work.

Concept and design: Sandeep P. Desai

Acquisition, analysis, or interpretation of data: Sandeep P. Desai

Drafting of the manuscript: Sandeep P. Desai

Critical review of the manuscript for important intellectual content: Sandeep P. Desai

Supervision: Sandeep P. Desai

Disclosures

Human subjects: All authors have confirmed that this study did not involve human participants or tissue.

Animal subjects: All authors have confirmed that this study did not involve animal subjects or tissue.

Conflicts of interest: In compliance with the ICMJE uniform disclosure form, all authors declare the following: **Payment/services info:** All authors have declared that no financial support was received from any organization for the submitted work. **Financial relationships:** All authors have declared that they have no financial relationships at present or within the previous three years with any organizations that might have an interest in the submitted work. **Other relationships:** All authors have declared that there are no other relationships or activities that could appear to have influenced the submitted work.

Acknowledgements

It is an invitation received from the organizers of the conference “Emerging Multifunctional Materials and Devices for Sustainable Technologies (IEMDST-2024),” organized by the Department of Physics, NIT Warangal, in association with the National Institute of Technology, Goa.

References

- Lewis BG, Paine DC: Applications and processing of transparent conducting oxides. *MRS Bulletin*. 2000, 25:22-27. [10.1557/mrs2000.147](https://doi.org/10.1557/mrs2000.147)
- Ingram BJ, Gonzalez GB, Kammler DR, Bertoni MI, Mason TO: Chemical and structural factors governing transparent conductivity in oxides. *Journal of Electroceramics*. 2004, 13:167-75. [10.1007/s10832-004-5094-y](https://doi.org/10.1007/s10832-004-5094-y)
- Minami T: Transparent conducting oxide semiconductors for transparent electrodes. *Semiconductor Science and Technology*. 2005, 20:S35-S44. [10.1088/0268-1242/20/4/004](https://doi.org/10.1088/0268-1242/20/4/004)
- Hayashi K, Matsuishi S, Kamiya T, Hirano M, Hosono H: Light-induced conversion of an insulating refractory oxide into a persistent electronic conductor. *Nature*. 2002, 419:462-65. [10.1038/nature01053](https://doi.org/10.1038/nature01053)
- Desai SP, Suryawanshi MP, Bhosale SM, Kim JH, Moholkar AV: Influence of growth temperature on the physico-chemical properties of sprayed cadmium oxide thin films. *Ceramics International*. 2015, 41:4867-73. [10.1016/j.ceramint.2014.12.045](https://doi.org/10.1016/j.ceramint.2014.12.045)
- Jefferson PH, Hatfield SA, Veal TD, King PDC, McConville CF, Zuniga-Perez J, Muñoz-Sanjósé V: Bandgap and effective mass of epitaxial cadmium oxide. *Applied Physics Letters*. 2008, 92:022101. [10.1063/1.2833269](https://doi.org/10.1063/1.2833269)
- Moholkar AV, Agawane GL, Sim KU, Kwon YB, Choi DS, Rajpure KY, Kim JH: Temperature dependent structural, luminescent and XPS studies of CdO:Ga thin films deposited by spray pyrolysis. *Journal of Alloys and Compounds*. 2010, 506:794-99. [10.1016/j.jallcom.2010.07.072](https://doi.org/10.1016/j.jallcom.2010.07.072)
- Dakhel AA: Bandgap narrowing in CdO doped with europium. *Optical Materials*. 2009, 31:691-95. [10.1016/j.optmat.2008.08.001](https://doi.org/10.1016/j.optmat.2008.08.001)
- Dakhel AA: Transparent conducting properties of samarium-doped CdO. *Journal of Alloys and Compounds*. 2009, 475:51-54. [10.1016/j.jallcom.2008.08.008](https://doi.org/10.1016/j.jallcom.2008.08.008)
- Dakhel AA: Correlated transport and optical phenomena in Ga-doped CdO films. *Solar Energy*. 2008, 82:513-19. [10.1016/j.solener.2007.12.004](https://doi.org/10.1016/j.solener.2007.12.004)
- Dakhel AA: Influence of hydrogenation on the electrical and optical properties of CdO:Tl thin films. *Thin Solid Films*. 2008, 517:886-90. [10.1016/j.tsf.2008.08.114](https://doi.org/10.1016/j.tsf.2008.08.114)
- Dakhel AA: Electrical and optical properties of iron-doped CdO. *Thin Solid Films*. 2010, 518:1712-15. [10.1016/j.tsf.2009.11.026](https://doi.org/10.1016/j.tsf.2009.11.026)
- Desai S, Suryawanshi MP, Gaikwad MA, Mane AA, Kim JH, Moholkar AV: Investigations on the thickness dependent structural, morphological, and optoelectronic properties of sprayed cadmium based transparent conducting oxide. *Thin Solid Films*. 2017, 628:196-202. [10.1016/j.tsf.2017.03.028](https://doi.org/10.1016/j.tsf.2017.03.028)
- Desai SP: Improved opto-electrical properties of spray deposited ytterbium doped cadmium oxide thin films. *Journal of Materials Science. Materials in Electronics*. 2018, 29:14416-26. [10.1007/s10854-018-9574-2](https://doi.org/10.1007/s10854-018-9574-2)
- Burstein E: Anomalous optical absorption limit in InSb. *Physical Review*. 1954, 93:632. [10.1103/PhysRev.93.632](https://doi.org/10.1103/PhysRev.93.632)
- Moss TS: The interpretation of the properties of indium antimonide. *Proceedings of the Physical Society. Section B*. 1954, 67:775. [10.1088/0370-1301/67/10/306](https://doi.org/10.1088/0370-1301/67/10/306)
- Thomas P, Abraham KE: Excitation wavelength dependent visible photoluminescence of CdO nanomorphotypes. *Journal of Luminescence*. 2015, 158:422-27. [10.1016/j.jlumin.2014.10.023](https://doi.org/10.1016/j.jlumin.2014.10.023)
- Sankarasubramanian K, Soundarrajan P, Sethuraman K, Ramamurthi K: Chemical spray pyrolysis deposition of transparent and conducting Fe doped CdO thin films for ethanol sensor. *Materials Science in*

- Semiconductor Processing. 2015, 40:879-84. [10.1016/j.mssp.2015.07.090](https://doi.org/10.1016/j.mssp.2015.07.090)
19. Haacke G: New figure of merit for transparent conductors . Journal of Applied Physics. 1976, 47:4086-89. [10.1063/1.323240](https://doi.org/10.1063/1.323240)